Electrocatalysis of Oxygen Reduction by Cu-containing Polymer Films on Glassy Carbon Electrodes

Jongwon Kim[*] and Andrew A. Gewirth[†]

Department of Chemistry, Chungbuk National University, Cheongju, Chungbuk 361-763, Korea
[*]E-mail: jongwonkim@chungbuk.ac.kr
[†]Department of Chemistry and Frederick Seitz Materials Research Laboratory, University of Illinois at Urbana-Champaign,
Urbana, IL 61801, USA

The catalytic activity of poly[(2,2'-bipyridine)copper(II)-μ_4-oxalato] coated on a glassy carbon electrode (GCE) for O_2 electroreduction is examined using cyclic voltammetry and rotating disk electrode techniques. The cyclic voltammograms show that O_2 is electroreduced on pBpCuOx-coated GCE surfaces at a peak potential of −0.25 V in pH 4.7 acetate buffer media. The electroreduction of O_2 on pBpCuOx-coated GCE occurs at 450 mV more positive potential than that found at a bare GCE. The catalytic activity originates from Cu(II) coordinated by bipyridine in the complexes and the polymer type Cu-complex films exhibit an enhanced stability compared to monomeric Cu-complexes during the O_2 electroreduction. The rotating disk electrode measurements reveal that the electroreduction of O_2 on pBpCuOx-coated GCE is a four-electron process. Kinetic parameters for O_2 reduction on pBpCuOx-coated GCE are obtained from rotating disk experiments and compared with those on bare glassy carbon electrode surfaces.

Key Words : Copper-containing polymer, Electrocatalysis, Oxygen reduction, Cyclic voltammetry, Rotating disk electrode

Introduction

Electroreduction of oxygen is one of the most important reactions in electrochemistry because of the central role it plays in fuel cell, corrosion, and industrial processes. The electrocatalytic reduction of oxygen has been extensively studied.[1,2] For bare metal surfaces, Pt (poly) is known to provide the best performance for the electroreduction of oxygen in acidic media. However, the high dissociation energy of O_2, 494 kJ·mol^{-1}, leads to slow kinetics and large overpotentials even on Pt. Additionally, the cost of Pt-including materials can be prohibitive. A major focus at present for oxygen electroreduction is replacing the precious-metal based catalysts currently used with those utilizing cheaper metals and featuring lower activation overpotentials.

Several different approaches have been examined over the past 40 years to circumvent Pt in low-temperature cathodes. These include (1) modification of the Pt material by alloying,[3] (2) modification of Pt or related precious metals by decoration of nanoparticles,[4,5] (3) use of bioinspired catalysts,[6-8] (4) use of combinatorial approaches,[9] and (5) use of transition metal based catalyst supported on graphite surfaces.[10,11] Among these approaches, transition-metal complexes have been widely investigated for the electrocatalysis of O_2 reduction. In particular, metallo-porphyrins adsorbed on graphite surfaces have shown unique catalytic activities for the electroreduction of O_2.[10,12-19] It was shown that dimeric cofacial cobalt porphyrins adsorbed on graphite surfaces catalyze the direct four-electron electroreduction of O_2.[12,18,19] The authors suggested that the mechanism of the

electrocatalytic reduction of O_2 involves the simultaneous interaction of two metal centers with two oxygen atoms of the O_2 molecules as the O-O bond is severed.[18] In the case of monomeric cobalt porphyrins, two-electron reduction of O_2 was observed.[15] However, four-electron reduction of O_2 could be achieved with monomeric cobalt porphyrins in some cases, which was ascribed to the strong tendency of the porphine to form dimeric, cofacially disposed rings through van der Waals interactions.[15] Interestingly, more recent studies show that some catalyst degradation likely occurs on the edge plane graphite electrode.[20,21] All of these studies imply the role of two metal centers in the electrocatalysis of O_2.

Recently, it was shown that cleavage of the O-O bond during the electroreduction of O_2 on Bi-modified Au(111) surfaces occurs only when the Bi adatoms are not close packed.[22,23] O_2 reduction activity is found only on the (2×2) Bi adlattice on Au(111), while the $(p \times \sqrt{3})$ Bi structure with a higher coverage is not catalytically active. The distance between two Bi atoms in the former structure is 6 Å, which apparently provides a proper spacing for O-O bond activation for the electroreduction of O_2. Interestingly, although the situation for the degraded edge plane graphite supported catalyst is more complex, Anson and Collman found the number of electrons as well as the onset potential associated with the electroreduction of O_2 is dependent on the distance between two Co atoms in supported dimeric Co porphyrin.[12]

The best oxygen reduction catalyst is the Cu trinuclear active site found in the protein laccase.[6,24,25] This observation, coupled with the insight that multimeric active sites
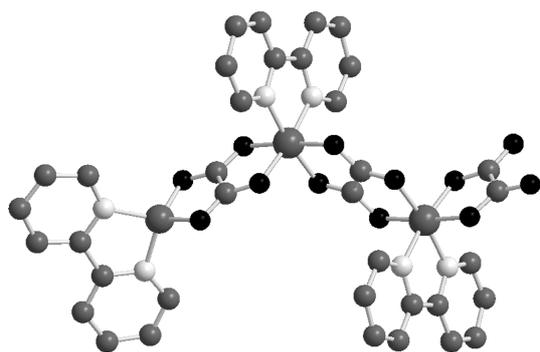
Figure 1. Structure of poly[(2,2'-bipyridine)copper(II)-μ_4-oxalato] (pBpCuOx). Cu atoms are represented by large gray circles, C atoms by small gray circles, N atoms by white circles, and O atoms by black circles.

exhibit the highest reactivity, leads us to examine dimeric Cu complexes. In this paper, we investigate the electrocatalytic activity of poly[(2,2'-bipyridine)copper(II)-μ_4-oxalato] (pBpCuOx) for O_2 reduction. The structure of pBpCuOx is shown in Figure 1. Each Cu atom is coordinated by a bipyridine group and bridged by an oxalate unit. The distance between two Cu atoms is 5.5 Å,[26] which is close to that between two Bi atoms in the catalytically active Bi-modified Au structures as previously reported.[22] The pBpCuOx films coated on glassy carbon electrode (GCE) surfaces shows catalytic activity for O_2 electroreduction. The pBpCuOx films are stable on GCE surfaces, while other metal complexes previously examined are not operational on this surface. Rotating disk electrode (RDE) experiments are utilized to evaluate kinetic parameters associated with O_2 reduction on pBpCuOx-modified GCE surfaces.

Experimental Procedures

All solutions were prepared using purified water (Milli-Q UV plus, 18.2 MΩ·cm). The supporting electrolyte was acetate buffer, prepared by partial neutralization of 0.1 M CH_3COOH (99.9985%, Alfa Aesar) to pH 4.7 with NaOH, or 0.1 M H_2SO_4 (J. T. Baker, Ultrapure reagent grade) solution. $CuCl_2$·$6H_2O$ (Fisher), tetrahydroxy-1,4-benzoqui-none (Aldrich), 2,2'-bipyridine (Aldrich), and methanol (Fisher) were used as received.

Poly[(2,2'-bipyridine)copper(II)-μ_4-oxalato] (pBpCuOx) was synthesized following published procedures.[26] A solution of $CuCl_2$·$6H_2O$ (0.5 mmol) and tetrahydroxy-1,4-benzoquinone (0.5 mmol) in methanol (20 mL) was stirred for 30 min at room temperature. 2,2'-bipyridine (0.5 mmol) was then added to this solution and the mixture was stirred for 1 h to give a green solution. The resulting solution was filtered and the remaining green solid was dried in air. pBpCuOx films were spin coated at 1000 rpm on glassy carbon electrode (GCE) from stock solutions of the pBpCuOx (10 mg) in methanol (10 mL) and dried in air for 10 min.

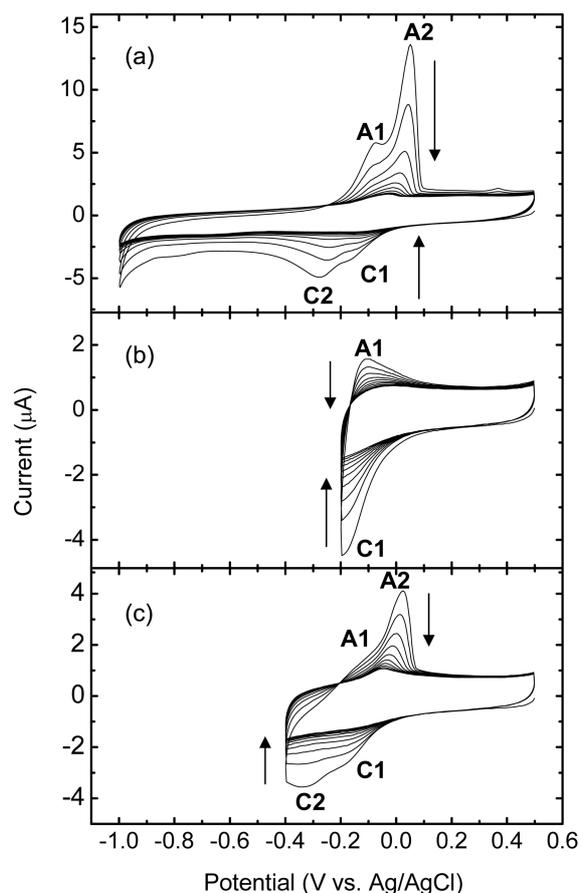Electrochemical measurements were conducted using a CHI 620A potentiostat (CH Instrument, Austin, TX) and the

Figure 2. Ten consecutive cyclic voltammograms of pBpCuOx-coated GCE in 0.1 M acetate buffer (pH 4.7) saturated with Ar with a negative potential limit of (a) -1.0 V, (b) -0.2 V, and (c) -0.4 V. Scan rate = 100 mV·s^{-1}.

solution was purged with Ar or O_2 prior to use. A commer-cially available GCE (diameter = 0.3 cm) (Bioanalytical Systems, West Lafayette, IN) was employed as the working electrode. Au wire and Ag/AgCl electrodes were used as counter and reference electrodes, respectively. All potentials are reported relative to the Ag/AgCl reference electrode (+0.20 V *vs.* NHE). For kinetic measurements, the working electrode was rotated using a Pine model MSRX rotator.

Results and Discussion

Electrochemical Behavior of pBpCuOx-Coated GCE. Figure 2a shows the time dependent cyclic voltammograms of pBpCuOx-coated GCE in 0.1 M acetate buffer saturated with Ar. The voltammograms show two cathodic waves at -0.16 V (C1) and -0.27 V (C2) and two anodic waves at -0.08 V (A1) and 0.05 V (A2). During ten consecutive cycles, the peak currents from these waves continuously decrease. After the tenth cycle, both of the cathodic and anodic waves disappear and only broad residual waves remain at ca -0.10 V and 0.025 V in the cathodic and anodic regions, respectively. To correlate the cathodic waves (C1 and C2) with their counterpart anodic waves, we performed the time dependent cyclic voltammetry with different

switching potentials. Figure 2b shows ten consecutive cyclic voltammograms with a negative potential limit of −0.2 V. This figure shows cathodic waves C1 and anodic waves A1, while no waves are observed related to the wave A2. When the negative potential limit is extended to −0.4 V (Figure 2c), we observe all the cathodic and anodic waves as shown in Figure 1a. Therefore, the cathodic wave C1 and C2 correspond to the anodic counter parts A1 and A2, respectively.

There are several previous reports examining the electrochemical response of Cu(II)-complexes of phenanthroline.[27-30] In these reports, Cu(II)-complexes coated on graphite surfaces exhibit redox waves corresponding to a Cu(II)/Cu(I) redox couple. Depending on the number of phenanthroline ligands, the Cu(II)/Cu(I) redox couple in the complex exhibits different reduction peak potentials. For example, Cu(II)-complexes bearing one phenanthroline ligand show more negative reduction potentials than those bearing two ligands.[28] In this study, we observe two redox waves from pBpCuOx films coated on GCE. There could be several explanations for the origin of the redox waves observed here. The redox wave C1/A1 can be assigned to Cu(II)/Cu(I) redox couple in the pBpCuOx films coated on GCE. This assignment is made on the basis of similar redox peak potentials in other Cu(II)-bipyridine complexes adsorbed on the graphite electrodes as reported previously.[27] For the other redox wave, C2/A2, the origin is unclear. The separation of peak potentials for the redox wave C2/A2 is 0.32 V, which is indicative of an irreversible redox process. One possibility could be that the Cu(II) in the polymers may loose some ligands during the electrochemical process, leading to a decrease in coordination number for the Cu(II) center and a consequent different redox potential. Another explanation for these redox waves could be that the reduced Cu(I) is further deposited as Cu(0) on the electrode surfaces. In this case the Cu(0) would no longer be coordinated by the bipyridine or oxalate ligands.

Electrocatalytic Activity of pBpCuOx-Coated GCE for O₂ Reduction. Figure 3a shows the first ten consecutive cyclic voltammograms for pBpCuOx-coated GCE in 0.1 M acetate buffer saturated with O_2. This figure exhibits cathodic waves for O_2 electroreduction at −0.25 V. For comparison, the cyclic voltammogram obtained on a bare GCE in the same O_2 saturated solution is shown as a dashed line. Compared with a bare GCE, O_2 is reduced at ca. 450 mV more positive potential at pBpCuOx-coated GCE electrodes. The anodic wave from pBpCuOx is observed at 0.05 V, which corresponds to the peak A2 in Figure 2a. Upon further potential cycling, this wave gradually decreases and disappears after 10 cycles. The decrease of catalytic current for O_2 electroreduction during the first ten cycles can be ascribed to the decrease in reduction current for pBpCuOx on GCE as shown above. However, the O_2 reduction currents remain at the same level in the next ten cycles as shown in Figure 3b, while the pBpCuOx films show no electrochemical activities after first ten potential cycles. The level of catalytic current for O_2 reduction
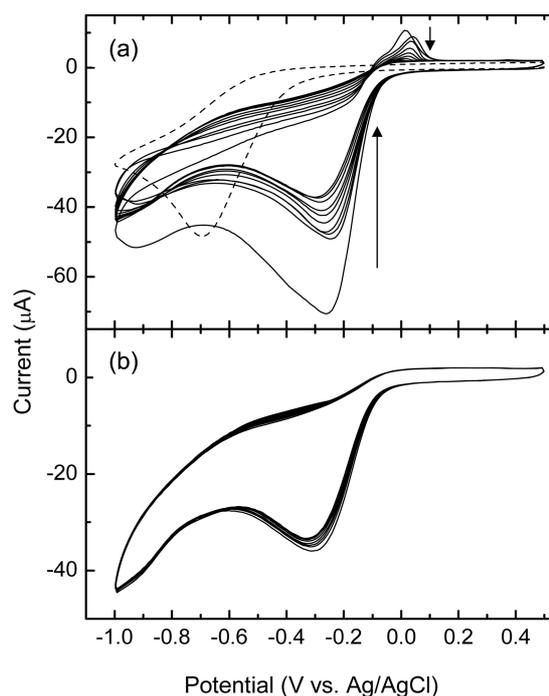

Figure 3. (a) First ten consecutive and (b) next ten consecutive cyclic voltammograms of pBpCuOx-coated GCE in 0.1 M acetate buffer (pH 4.7) saturated with O_2. The dashed line was obtained on a bare GCE in the same solution. Scan rate = 100 mV·s^{-1}.

persists at least for ca. 20 further potential cycles.

Anson and co-workers reported several papers investigating the electrocatalytic activity of Cu(II)-complexes adsorbed on edge-plane pyrolytic graphite (EPG) surfaces for the electroreduction of O_2.[27-29,31,32] For example, the half wave potential of O_2 reduction at Cu(II)-bipyridine adsorbed EPG surfaces is −0.2 V at pH 5.[27] The reduction potential for O_2 reduction on pBpCuOx-coated GCE in 0.1 M acetate buffer (pH 4.7) is close to this value as shown in Figure 2. In a previous study on Cu(II)-complexes adsorbed on EPG surfaces, the potential shifts for O_2 electroreduction between modified and bare EPG electrodes were reported to be ca. 200 mV.[31,32] There is another report on the electrocatalytic behavior of Cu(II)-phenanthroline complexes for O_2 electroreduction on GCE surfaces, where the enhancement in peak potential for O_2 reduction was around 300 mV.[30] The pBpCuOx-coated GCE system used in this report shows better catalytic enhancement for O_2 electroreduction that those reported previously.

Next we examined the catalytic activity of pBpCuOx-coated GCE for O_2 reduction in 0.1 M H_2SO_4 solution, which has a lower pH than the acetate buffer solution. Figure 4 shows the cyclic voltammograms from pBpCuOx-coated GCE in O_2-saturated 0.1 M H_2SO_4. The thin solid line in Figure 4a corresponds to the first potential cycle. The peak potential of O_2 reduction is −0.15 V, which is 100 mV more positive than that observed in acetate buffer. Upon further potential cycling, the currents for O_2 reduction decrease gradually as shown in Figure 4b. In contrast to the cyclic voltammograms obtained in acetate buffer shown in Figure
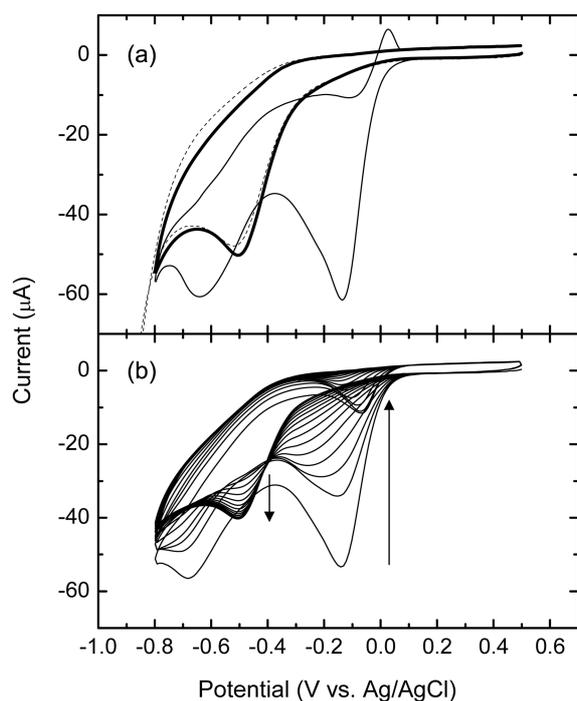
Figure 4. Cyclic voltammograms of pBpCuOx-coated GCE in 0.1 M H$_2$SO$_4$ saturated with O$_2$. (a) First (thin solid line) and seventeenth (thick solid line) cycles. (b) Consecutive cycles between second and sixteenth cycles. The dashed line was obtained on a bare GCE in the same solution. Scan rate = 100 mV·s^{-1}.

3a, a new cathodic wave develops at −0.5 V and increases upon further potential cycling. The thick solid line in Figure 4a was obtained after 15 consecutive potential cycles, where the catalytic current at −0.15 V disappears and a new wave for O$_2$ reduction is observed at −0.5 V. This cyclic voltam-mogram is the same as that obtained on a bare GCE in 0.1 M H$_2$SO$_4$ saturated with O$_2$ as shown in Figure 4a (dashed line). This indicates that the pBpCuOx films on GCE surfaces are not stable in 0.1 M H$_2$SO$_4$ media during the electroreduction of O$_2$. Compared with a bare GCE in this media, O$_2$ is reduced at ca. 350 mV more positive potential on pBpCuOx-coated GCE electrodes. The potential enhan-cement in electrocatalytic reduction of O$_2$ by pBpCuOx in 0.1 M H$_2$SO$_4$ is smaller than that found in 0.1 M acetate buffer solution. Considering the magnitude of catalytic enhancement as well as the stability of films during the electroreduction of reduction of O$_2$, we elected to use acetate buffer as supporting electrolyte solutions in subsequent investigations.

Rotating Disk Electrode (RDE) Experiments. To in-vestigate the kinetics of O$_2$ electroreduction on pBpCuOx-coated GCE, we performed rotating disk electrode (RDE) measurements. Figure 5a shows the RDE voltammograms of pBpCuOx-coated GCE in 0.1 M acetate buffer saturated with O$_2$ at various rotating rates. The currents associated with O$_2$ reduction begin to flow around −0.1 V and exhibit plateaus after *ca.* −0.4 V at rotation rates up to 600 rpm. Figure 5b shows the relationship between the O$_2$ reduction current and the square of the rotation rate at −0.4 V. The
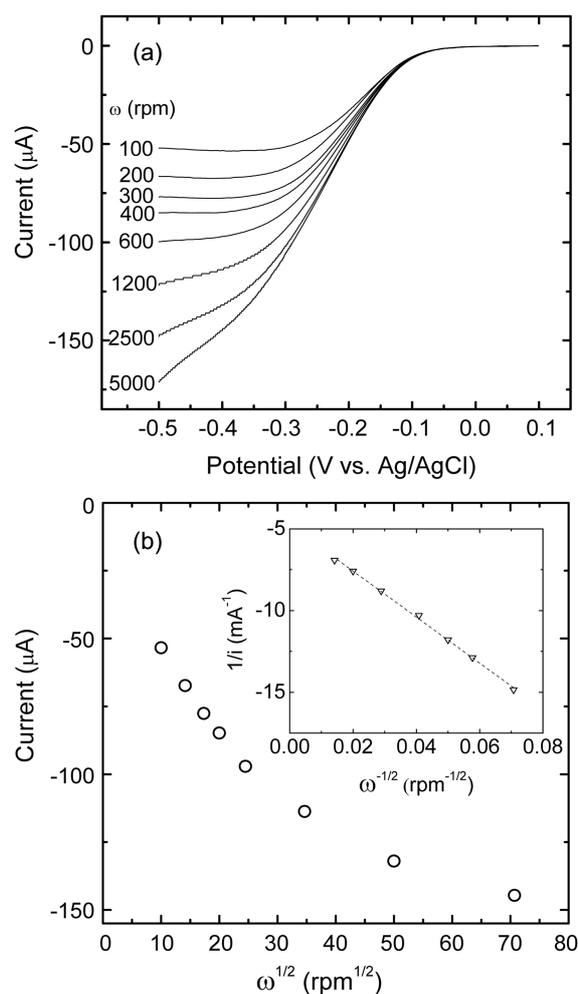

Figure 5. (a) RDE voltammograms of pBpCuOx-coated GCE in 0.1 M acetate buffer saturated with O$_2$ at various rotation rates. Scan rate = 25 mV·s^{-1}. (b) Plot of the current at −0.4 V as a function of the square root of the rotation rate. The inset is Koutechy-Levich plot obtained from the RDE voltammograms in Figure 5a at −0.4 V.

currents increase linearly up to the rotation rate of 600 rpm, after which the current exhibits a negative deviation. This means that the O$_2$ electroreduction process on pBpCuOx-coated GCE is controlled by both mass transfer and electrode kinetics.[33]

For electrode processes with slow kinetics, the Koutechy-Levich equation applies, and the current (*i*) can be expressed as[33]

$$\frac{1}{i} = \frac{1}{i_K} + \frac{1}{0.62nFAD_0^{2/3}\omega^{1/2}v^{-1/6}C_0} \qquad (1)$$

where i_K is the kinetic current in the absence of mass-transfer effect; n is the number of electrons exchanged in the O$_2$ reduction reaction; F is the Faraday constant; A is electrode area; D_o is the diffusion coefficient of O$_2$ (1.9 × 10^{-5} cm^{-1} s^{-1})[34]; ω is the rotation rate; v is the kinematic viscosity (9.97×10^{-5} cm^2 s^{-1});[34] and C_o is the bulk concentration of O$_2$ (1.1×10^{-6} mol cm^{-3} at pH 4.7).[13] The inset of Figure 5b shows the Koutechy-Levich plot obtained

from the RDE voltammograms shown in Figure 5a. From this plot the number of electrons exchanged in the O_2 reduction reaction, *n* is calculated to be 3.6, which indicates the catalytic reduction of O_2 on pBpCuOx-coated GCE surfaces is four-electron process. The number of electrons associated with the O_2 reduction on a bare GCE is known to be around 2.[35] In previous work, both two-[31,32] and four-electron[27] reduction of O_2 on Cu(II)-complex adsorbed EPG surfaces were found. The extrapolated Koutechy-Levich plot for $\omega^{-1/2} = 0$ has an intercept other than zero, which indicates a mixed kinetic-diffusion controlled mechanism.[36] From the intercept in the Koutechy-Levich plot, we can evaluate the $1/i_K$ values at differential potentials and the i_K value is further expressed as

$$i_K = FAk_0(E^{0'})C_0 \qquad (2)$$

where we can determine the standard rate constant k_0.[33] The k_0 value for O_2 reduction on pBpCuOx-coated GCE is found to be 2×10^{-3} cm s^{-1}. This rate constant for O_2 electro-reduction is somewhat larger than that found on a bare GCE which is known to be *ca.* 5×10^{-4} cm s^{-1}.[36] The pBpCuOx films on GCE surfaces convert the number of electrons for O_2 reduction from 2 to 4 and enhance the reaction kinetics compared to those observed on a bare GCE.

Origin of Electrocatalytic Activity. Next we examine the origin of the catalytic activity for O_2 reduction on pBpCuOx-coated GCE. First we test the possibility of catalytic action of Cu atoms deposited on GCE during the electrochemical reduction process. Figure 6 shows cyclic voltammograms of a bare GCE in 1 mM $CuCl_2$ + 0.1 M acetate buffer in the absence and presence of O_2. The cathodic wave at -0.1 V corresponds to Cu deposition on GCE, while anodic Cu dissolution wave appears at 0.15 V. In the presence of O_2, the current at -0.1 V slightly increases, but most of O_2 reduction occurs at -0.7 V, at which potential O_2 is reduced on a bare GCE electrode as indicated in Figure 3. Thus Cu deposited on GCE has little catalytic effect on O_2 electroreduction. We also checked a possibility of catalytic effect for O_2 electroreduction from tetrahydroxy-1,4-
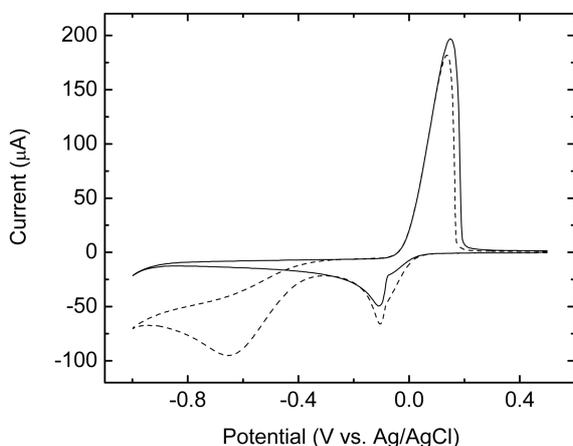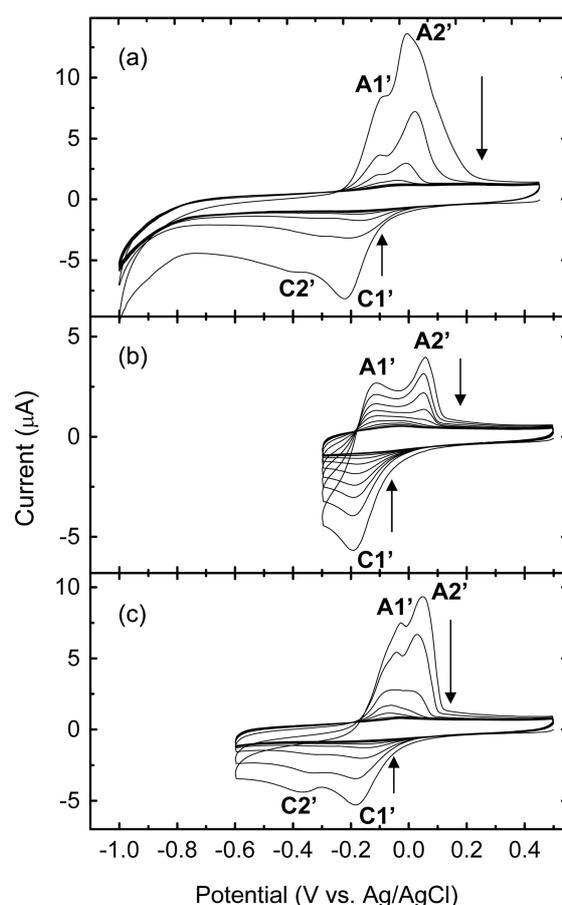

Figure 7. Ten consecutive cyclic voltammograms of BpCu-coated GCE in 0.1 M acetate buffer (pH 4.7) saturated with Ar with a negative potential limit of (a) -1.0 V, (b) -0.3 V, and (c) -0.6 V. Scan rate = 100 mV·s^{-1}.

benzoquinone or $CuCl_2$ + tetrahydroxy-1,4-benzoquinone in solution phase, but no catalytic activity was observed.

We also investigated the catalytic activity of Cu(II)-bipyridine complex (CuBp) coated on GCE for electro-reduction of O_2. A solution containing 5 mg of $CuCl_2$ and 5 mg 2,2'-bipyridine in 10 mL MeOH was prepared, and then a GCE was spin coated in this solution and dried for 10 min. Figure 7 shows the cyclic voltammograms of BpCu-coated GCE in 0.1 M acetate buffer saturated with Ar. In Figure 7a, two cathodic waves at -0.2 V (C1') and -0.35 V (C2') and two anodic waves at -0.05 V (A1') and 0.05 V (A2') are observed. The peak position of these redox couples are close to those found at pBpCuOx-coated GCE. During ten consecutive cycles, the peak currents continuously decrease as the case of pBpCuOx-coated GCE. However, after tenth cycle, both of the cathodic and anodic waves completely disappear and no residual current remains. Figure 7b and 7c show ten consecutive cyclic voltammograms with switching potentials of -0.3 and -0.6 V, respectively. In contrast to the electrochemical response of pBpCuOx-coated GCE, the cathodic wave C1' of the Cu(II)-bipyridine complex is responsible for two anodic waves (A1' and A2'). There seems to be no clear explanation for this behavior. This
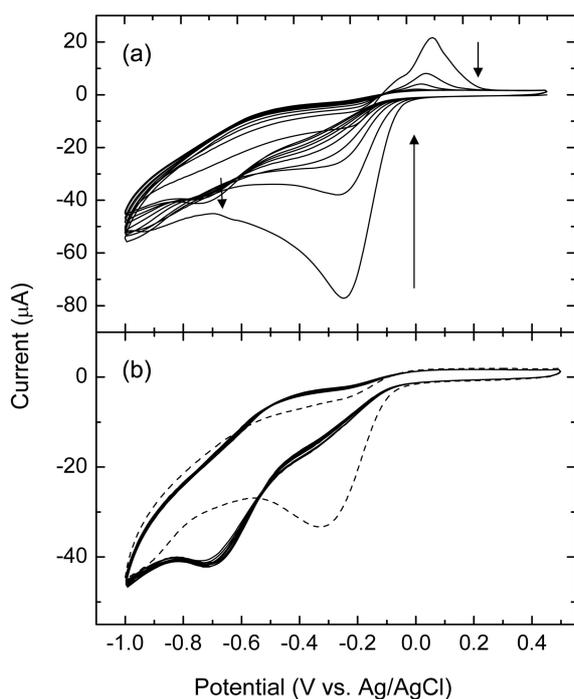

Figure 6. Cyclic voltammograms of a bare GCE in in 1 mM $CuCl_2$ + 0.1 M acetate buffer (pH 4.7) saturated with Ar (solid line) and O_2.(dashed line). Scan rate = 100 mV·s^{-1}.

Figure 8. (a) First ten consecutive and (b) next ten consecutive cyclic voltammograms of BpCu-coated GCE in 0.1 M acetate buffer (pH 4.7) saturated with O_2. Dashed line was obtained on pBpCuOx-coated GCE in 0.1 M acetate buffer (pH 4.7) saturated O_2 after 20 consecutive potential cycles. Scan rate = 100 mV·s^{-1}.

might indicate a special role for oxalate groups in the electrochemical behavior of pBpCuOx films on GCE.

Figure 8a shows the cyclic voltammograms of BpCu-coated GCE in 0.1 M acetate buffer saturated with O_2. The BpCu-coated GCE shows catalytic activity for O_2 reduction at −0.25 V. During the consecutive potential cycles, the catalytic currents quickly decrease. After 10 potential cycles, catalytic activity almost disappears and the electrode exhibits the characteristics of a bare GCE. The peak potential for O_2 reduction on BpCu-coated GCE is the same as that observed on pBpCuOx-coated GCE. The catalytic activity of BpCu on O_2 electroreduction has been already reported in previous study, where BpCu complexes absorbs on pyrolytic graphite surfaces and the catalytic activity is maintained.[27] In our case, monomeric BpCu complexes do not adsorbed on GCE surfaces so catalytic activity is quickly lost.

Figure 8b compares the catalytic currents of CuBp-coated and pBpCuOx-coated GCEs for O_2 electroreduction after 20 consecutive potential cycles. Redox waves from Cu-complexes disappear after *ca.* 10 cycles in both cases; however, the catalytic activity shows different time dependence. After 20 potential cycles, pBpCuOx-coated GCE still exhibits O_2 reduction wave at −0.3 V, while BpCu-coated GCE loses most of catalytic activity. The use of polymers instead of monomeric Cu-complexes increases the stability of films on GCE. The role of oxalate in the catalysis of O_2 electroreduction is unclear and will be the subject of future study.

Finally we also attempted to utilize other first-row transi-

tion metals for polymer synthesis. The same procedure as used for pBpCuOx was employed to synthesize polymers containing Fe(III), Co(II), Ni(II), and Zn(II) and their electrocatalytic activity for O_2 reduction was tested. However, all of these polymers do not exhibit catalytic activities compared to that found in Cu-containing polymers, which indicates a unique role of Cu in the polymer coated on electrodes for O_2 electroreduction.

Conclusions

The catalytic activity of poly[(2,2'-bipyridine)copper(II)-μ_4-oxalato] (pBpCuOx) coated on GCE for O_2 electroreduction was investigated. O_2 is electroreduced on pBpCuOx-coated GCE at 450 mV more positive potential than that found at a bare GCE. The catalytic enhancement for O_2 electroduction is better than that reported previously. The number of electrons associated with O_2 reduction on pBpCuOx-coated GCE was found to 4. This polymer type Cu-complex films show a better stability than monomeric Cu-complexes. The kinetic parameters for O_2 reduction on pBpCuOx-coated GCE were obtained from rotating disk experiments and compared with those on bare glassy carbon electrode surfaces.

References

1. Tarasevich, M. R.; Sadkowski, A.; Yeager, E. In *Comprehensive Treatise of Electrochemistry*; Conway, B. E., Bockris, J. O. M., Yeager, E., Kahn, S. U. M., White, R. E., Eds.; Plenum: New York, 1983; Vol. 7, p 301.
2. Adzic, R. R. In *Electrocatalysis*; Lipkowski, J., Ross, P. N., Eds.; Wiley-VCH: New York, 1998; p 197.
3. Mukerjee, S.; Srinivasan, S.; Soriaga, M. P.; McBreen, J. *J. Phys. Chem.* **1995**, *99*, 4577.
4. Schmidt, T. J.; Stamenkovic, V.; Arenz, M.; Markovic, N. M.; Ross, P. N. *Electrochim. Acta* **2002**, *47*, 3765.
5. Zhang, J.; Mo, Y.; Vukmirovic, M. B.; Klie, R.; Sasaki, K.; Adzic, R. R. *J. Phys. Chem. B* **2004**, *108*, 10955.
6. Solomon, E. I.; Sundaram, U. M.; Machonkin, T. E. *Chem. Rev.* **1996**, *96*, 2563.
7. Mano, N.; Fernandez, J. L.; Kim, Y.; Shin, W.; Bard, A. J.; Heller, A. *J. Am. Chem. Soc.* **2003**, *125*, 15290.
8. Soukharev, V.; Mano, N.; Heller, A. *J. Am. Chem. Soc.* **2004**, *126*, 8368.
9. Fernandez, J. L.; Walsh, D. A.; Bard, A. J. *J. Am. Chem. Soc.* **2005**, *127*, 357.
10. Collman, J. P.; Marrocco, M.; Denisevich, P.; Koval, C.; Anson, F. C. *J. Electroanal. Chem.* **1979**, *101*, 117.
11. Park, H.; Kwon, T. G.; Park, D. S.; Shim, Y. B. *Bull. Korean Chem. Soc.* **2006**, *27*, 1763.
12. Collman, J. P.; Denisevich, P.; Konai, Y.; Marrocco, M.; Koval, C.; Anson, F. C. *J. Am. Chem. Soc.* **1980**, *102*, 6027.
13. Shigehara, K.; Anson, F. C. *J. Phys. Chem.* **1982**, *86*, 2776.
14. Shi, C. N.; Mak, K. W.; Chan, K. S.; Anson, F. C. *J. Electroanal. Chem.* **1995**, *397*, 321.
15. Shi, C.; Steiger, B.; Yuasa, M.; Anson, F. C. *Inorg. Chem.* **1997**, *36*, 4294.
16. Song, E. H.; Shi, C. N.; Anson, F. C. *Langmuir* **1998**, *14*, 4315.

17. Steiger, B.; Anson, F. C. *Inorg. Chem.* **2000**, *39*, 4579.
18. Anson, F. C.; Shi, C. N.; Steiger, B. *Acc. Chem. Res.* **1997**, *30*, 437.
19. Chang, C. J.; Loh, Z. H.; Shi, C. N.; Anson, F. C.; Nocera, D. G. *J. Am. Chem. Soc.* **2004**, *126*, 10013.
20. Lefevre, M.; Dodelet, J. P.; Bertrand, P. *J. Phys. Chem. B* **2005**, *109*, 16718.
21. Lefevre, M.; Dodelet, J. P.; Bertrand, P. *J. Phys. Chem. B* **2002**, *106*, 8705.
22. Li, X.; Gewirth, A. A. *J. Am. Chem. Soc.* **2003**, *125*, 7086.
23. Li, X.; Gewirth, A. A. *J. Am. Chem. Soc.* **2005**, *127*, 5252.
24. Lee, C. W.; Gray, H. B.; Anson, F. C.; Malmstrom, B. G. *J. Electroanal. Chem.* **1984**, *172*, 289.
25. Barton, S. C.; Kim, H. H.; Binyamin, G.; Zhang, Y. C.; Heller, A. *J. Am. Chem. Soc.* **2001**, *123*, 5802.
26. Luo, J. H.; Hong, M. C.; Liang, Y. C.; Cao, R. *Acta Crystallogr. Sect. E.-Struct Rep. Online* **2001**, *57*, M361.
27. Zhang, J. J.; Anson, F. C. *Electrochim. Acta* **1993**, *38*, 2423.
28. Lei, Y. B.; Anson, F. C. *Inorg. Chem.* **1994**, *33*, 5003.
29. Lei, Y. B.; Anson, F. C. *Inorg. Chem.* **1995**, *34*, 1083.
30. Liu, S. J.; Huang, C. H.; Chang, C. C. *Mater. Chem. Phys.* **2003**, *82*, 551.
31. Zhang, J. J.; Anson, F. C. *J. Electroanal. Chem.* **1992**, *341*, 323.
32. Zhang, J. J.; Anson, F. C. *J. Electroanal. Chem.* **1993**, *348*, 81.
33. Bard, A. J.; Faulkner, L. R. *Electrochemical Methods*, 2nd ed.; John Wiley & Sons: New York, 2001.
34. Tamura, K.; Ocko, B. M.; Wang, J. X.; Adzic, R. R. *J. Phys. Chem. B* **2002**, *106*, 3896.
35. Vaik, K.; Schiffrin, D. J.; Tammeveski, K. *Electrochem. Commun.* **2004**, *6*, 1.
36. Tammeveski, K.; Kontturi, K.; Nichols, R. J.; Potter, R. J.; Schiffrin, D. J. *J. Electroanal. Chem.* **2001**, *515*, 101.